Fungal polysaccharopeptides reduce obesity by richness of specific microbiota and modulation of lipid metabolism

Xiaojun Li, Peng Chen, Peng Zhang, Yifan Chang, Mingxu Cui and Jinyou Duan*

Shaanxi Key Laboratory of Natural Products & Chemical Biology, College of Chemistry & Pharmacy, Northwest A&F University, Yangling 712100, Shaanxi, China

* Correspondence:

Jinyou Duan, PhD

Tel.: +86 29-87092662;

E-mail: jduan@nwsuaf.edu.cn

Keywords: *Coriolus versicolor*; Protein-bound β-glucan; Obesity; Gut microbiota; *Akkermansia muciniphila*; Lipid metabolism

Abstract

The prevalence of obesity and related disorders has vastly increased throughout the world and prevention of such circumstances thus represents a major challenge. Here, we show that protein-bound β-glucan (PBG), one representative of *Coriolus versicolor* polysaccharopeptides which are broadly used as immune boosters and clinically implicated in treatment of cancers and chronic hepatitis, could be a potent anti-obesity agent. PBG could reduce obesity and metabolic inflammation in mice fed with a high-fat diet (HFD). Gut microbiota analysis revealed that PBG markedly increased the abundance of *Akkermansia muciniphila* although it didn't rescue HFD-induced change in the *Firmicutes* to *Bacteroidetes* ratio. It appeared that PBG altered host physiology and created an intestinal microenvironment favorable for *A. muciniphila* colonization. Fecal transplants from PBG-treated animals in part reduced obesity in recipient HFD-fed mice. Further, PBG was shown to promote lipid metabolism in microbiota-depleted mice. Thus, our data highlights that PBG might exert its anti-obesity effects through a mirobiota-dependent (richness of specific microbiota) and -independent (modulation of lipid metabolism) manner. The fact that *Coriolus versicolor* polysaccharopeptides are approved oral immune boosters in cancers and chronic hepatitis with well-established safety profiles may accelerate the development of PBG as a novel drug for obesity treatment.

Introduction

Obesity, an abnormal or excessive fat accumulation in adipose tissues, has become a major public health issue worldwide. Obesity is well-known as a contributing factor in diabetes, cardiovascular disease, hypertension, stroke, and cancer, etc (1). Given the serious health consequences of obesity as well as its economic burden, greater attention must be directed to the prevention, identification, and treatment of overweight and obese conditions (2).

Despite the fact that dieting and physical exercise is the main treatment modalities, persons with obesity failing lifestyle therapies need further aggressive intervention including pharmacotherapy, medical devices and bariatric surgery (3-5). Noninvasive anti-obesity drugs have resurfaced as adjunctive therapeutic approaches to bridge a gap between intensive lifestyle intervention and surgery (6).

Drug repurposing, also known as drug repositioning, is a strategy that seeks to reuse existing, licensed medications for new medical indications (7). It offers a variety of advantages when compared with *de novo* drug development. These include the availability of extensive pharmacokinetic, pharmacodynamic and safety data, and an understanding of relevant molecular targets and mechanisms of action, due to previous considerable clinical experience (8). Thus, drug repurposing can greatly slash development costs and quickly translate those existing medications into treatment of epidemic or devastating diseases (9).

Many cultures worldwide have long recognized that hot water decoctions from certain medicinal mushrooms such as *Ganoderma lucidum* and *Coriolus versicolor*

have health-promoting benefits (10). Thereinto, the polysaccharide fractions are believed as the major immunotherapeutic components, which are either β-glucans, β-glucans with heterosaccharide chains or protein-bound β-glucans (PBGs), in other words, polysaccharopeptides (11-13). Numerous investigations *in vitro*, *in vivo* and clinical trials have reported that crude or purified PBGs from *C. versicolor* were adopted as an adjunct therapy for cancer (14) or chronic hepatitis (15). In this study, one purified PBG was repositioning as a potent anti-obesity agent and the in-depth understanding of this beneficial effect was examined.

Results

PBG prevents HFD-induced obesity

Oral administration of PBG daily at either a low dose (200 mg/kg, Group L) or a high dose (400 mg/kg, Group H) leads to a significant decrease of body weight in HFD-fed mice from 5 to 9 weeks (Fig.1a). The decreased weight gain (Fig.1b) and liver weight (Fig.1c) in PBG-treated mice at 9 weeks is not due to reduced food consumption (Fig.1d). PBG substantially prevents HFD-induced fat accumulation (Fig.1e), while it has no effect on lean mass (Fig.1f). Magnetic resonance imaging (MRI) reveals that PBG treatment apparently attenuates fat area in HFD-fed mice (Fig.1gh). Consistent with macroscopic evaluation of adiposity above, PBG feeding results in a dramatic reduction of triglyceride contents (Fig.1i), total bile acid (Fig.1j) and leptin (Fig.1k) in serum. There is an increase of plasma adiponectin (Fig.1l) and a decrease of hepatic lipid droplets (Fig.1mn) in HFD-fed mice after PBG treatment. It is noted that PBG daily at a dose of 200 mg/kg elicits an anti-obesity effect, comparable to simvastatin (2 mg/kg), a lipid-lowering medication on the World Health Organization's List of Essential Medicines while it is believed to be contraindicated with pregnancy, breast feeding, and liver disease (16).

PBG reduces obesity-related metabolic inflammation

Obesity is always associated with a low-grade chronic inflammation (17). HFD-fed mice produce higher levels of pro-inflammatory cytokines including tumors necrosis factor-alpha (TNF-α), interleukin-1-beta (IL-1β), interleukin-17A (IL-17A) and interleukin-6 (IL-6) in serum than chow-fed mice do (Fig.2a-d), indicating the

92 systemic inflammation is induced by HFD feeding. Administration of PBG or
93 simvastatin suppresses the overproduction of those pro-inflammatory cytokines above
94 in HFD-fed mice.

95 The obesity-related inflammation is characterized with an elevated level of gut
96 microbiota-derived lipopolysaccharide (LPS) in circulation, an event defined as
97 metabolic endotoxemia (18). PBG or simvastatin significantly reduces serum LPS
98 levels in HFD-fed mice (Fig.2e), and increases expression of the tight junction
99 components, zonula occludens-1 (ZO-1) (Fig.2f) and occludin-1 (Fig.2g). It seems that
100 PBG can upregulate the transcription of ZO-1 and occluding-1 in microbiota-depleted
101 mice, suggesting PBG directly protects HFD-induced disruption of tight junction
102 regardless of gut microbiota (Fig.2h). The findings above are consistent with the
103 concept that the increased expression of intestinal tight junction proteins improves
104 intestinal barrier integrity and thus decreases leakage of microbial LPS from gut into
105 circulation (17).

106 **PBG beneficially alters obese-type gut microbiota**

107 It is generally accepted that changes in the composition of gut microbiota are
108 associated with the development of obesity (19). To assess whether gut microbiota is
109 involved in the anti-obesity effects of PBG, we performed a pyrosequencing-based
110 assay of bacterial 16S rRNA (V3-V4 region) in fecal samples from different groups of
111 mice (11-13 mice/group). After removing unqualified sequences (see Methods), a total
112 of 4,799,464 raw reads and an average of 67,738±3,949 reads per sample were
113 obtained. After selecting the effective reads, a total of 3,244,442 effective reads was

114 generated and each fecal sample produced an average of 54,074±4,309 effective reads.
115 Samples with a low number of effective reads (<1622) were not observed. High-quality
116 reads were clustered into Operational Taxonomic Units (OTUs).

117 Principal coordinates analysis (PCoA) of unweighted UniFrac distances of fecal
118 microbiota was plotted, based on OTU abundances (Fig. 3a). The PCoA scores clearly
119 display a distinct clustering of microbiota composition for each treatment group.
120 Simvastatin treatment induces a mild shift of gut microbiota in HFD-fed mice, while
121 intake of PBG leads to a more pronounced change in microbiota composition. The
122 UPGMA (unweighted pair-group method with arithmetic means) tree also indicates
123 there is a remarkable separation between the microbiota from most mice for each
124 treatment (Fig. 3b).

125 Analysis of bacterial relative abundance confirmed prior reports that gut microbial
126 communities of mice are dominated by bacteria from the *Firmicutes* and *Bacteroidetes*
127 phyla (Fig. 3b) and that HFD feeding increases the proportion of *Firmicutes* versus
128 *Bacteroidetes* (20). It appear that either PBG or simvastatin treatment doesn't rescue
129 HFD-induced change in the *Firmicutes* to *Bacteroidetes* ratio (Fig. 3c). The most
130 striking difference in gut microbiota between HFD-fed mice and PBG-treated mice lies
131 in the abundance of the phylm *Verrucomicrobia* (Fig. 3c).

132 We used Wilcoxon signed-rank test to identify the specific bacterial genera that
133 were altered by HFD feeding and PBG treatment (Fig. 3d). Compared with chow-fed
134 mice, HFD feeding significantly altered 420 OTUs, producing 249 increased and 171
135 decreased OTUs. In HFD-fed mice, simvastatin treatment altered 36 OTUs (13

136 increased and 23 decreased), while PGB daily at a dose of 400 mg/kg altered 140
137 OTUs (29 increased and 111 decreased). Detailed analysis of the Top 100 OTUs
138 indicated that the following 4 genera, *Akkermansia*, *Bacteroides*, *Bacterium*, and
139 *Ruminiclostridium_10* were profoundly increased in PBG-treated HFD-fed mice. The
140 most striking one was *Akkermansia,* which was identified as the sole genus in the
141 phylm *Verrucomicrobia*. PBG increased the percentage of *Akkermansia* from 5.67 ±
142 1.5% to 22.1 ± 2.3% ($p < 0.0001$) at a daily dose of 400 mg/kg.

143 **PBG promotes *Akkermansia muciniphila* colonization through altered host**
144 **physiology**

145 It remains to be determined whether the interaction between PBG and the gut
146 microbiota, *Akkermansia* is direct or indirect (i.e., mediated through promoting
147 bacterial growth or altering host physiology). The *in vitro* analysis indicated that PBG
148 couldn't directly promote the growth of *A. muciniphila* in the pure culture (Fig.4a). To
149 see whether PBG affected the growth of *A. muciniphila* in a complex microbiota, we
150 cultured fecal samples supplemented with *A. muciniphila* in two separate
151 gut-simulators, and exposed them to a constant flow of PBG (40 mg/mL) for 42 h. No
152 substantial difference in the abundance of *A. muciniphila* was observed following PBG
153 exposure (Fig.4b).

154 To address whether PBG could alter host physiology and thus facilitate *A.*
155 *muciniphila* colonization, we treated mice with an antibiotic cocktail for one month to
156 deplete gut microbiota. The microbiota-depleted mice were further treated daily with
157 PBG or PBS, along with the antibiotic cocktail to prevent recurrence of microbiota for

158 another month. The mice were lavaged with *A. muciniphila* (2×10^8 cfu / 0.2ml)
159 continuously for 3 days and its abundance in the fecal samples was determined 24 h
160 after each lavage. The amount of *A. muciniphila* was statically different at day 3 in
161 feces between PBG-treated mice and control mice (Fig.4c).This observation suggested
162 that PBG created an intestinal microenvironment favorable for *A. muciniphila*
163 colonization.

164 *A. muciniphila* degrades intestinal mucins, the highly glycosylated proteins of the
165 epithelial mucus layer, as its preferred source of carbon and nitrogen (21). Alterations
166 of the mucus could be caused either by modification of gene expression that encode for
167 the mucins (MUC genes) and/or of genes encoding for glycosyltransferases (GT genes)
168 (22-24). We did not observe significant differences in gene expression of mucin 2
169 protein (encode by MUC2 gene) and its related glycosyltransferases (C1galt1 and
170 C2gnt genes) in colon tissues from PBG-treated mice and control mice (Fig.4d),
171 suggesting that *A. muciniphila* is not simply responding to increased host mucin
172 production.

173 **Fecal microbiota transplantation from PBG-treated mice reduces obesity**

174 It is well-known that alteration of gut microbiota by the transfer of foreign fecal
175 materials could modulate obesity (25). We daily transferred fecal microbiota from the
176 donor mice including chow-fed one, PBG treated chow-fed one, PBG treated HFD-fed
177 one and HFD-fed one to the recipient HFD-fed mice. After 8 weeks, obesity-related
178 syndromes were examined. The fecal transfer from the donor mice fed with chow
179 (Chow→HFD), chow and PBG [PBG(Chow)→HFD], or HFD and PBG [PBG

(HFD)→HFD] reduced body weight, plasma leptin and total bile acid and increased plasma adiponectin, compared with that from HFD-fed mice (HFD→HFD) (Fig. 5a–c). Correspondingly, the obesity-related metabolic inflammation, as indicated by elevated serum levels of proinflammatory cytokines such as IL-6, IL-1β and TNF-α in the recipient mice was also diminished after the first three fecal microbiota transplantation above (Fig. 5d–f). These results suggest that the anti-obesity effects of PBG in HFD-fed mice might be due to modulation of the gut microbiota.

PBG directly upregulates a set of gene expression involved in host metabolism

To find out whether PBG has a direct impact on host metabolism, we performed transcriptomic analysis of colon tissues from microbiota-depleted mice treated with or without PBG. After quality control, a total of 130,093,406 clean reads and 38.78 Gb clean bases were obtained. The percentage of Q30 bases in each sample was not less than 90.94%. A total of 22,419 UniGenes were identified. To facilitate the functional analysis of these RNAs, the differential expressed mRNA genes were picked from the whole gene matrix with Cuffdiff (26) according to the two standards: |log2(Fold Change)| ≧ 1 and adjusted *p*-value < 0.05. Compared with the control group, the PBG group had 155 differential expressed genes (DEGs) (Fig. 6a). Among 155 DEGs, 120 were successfully annotated by Gene Ontology (GO) assignments and classified into three functional categories, which were molecular function, biological process, and cellular component. There were less DEGs classified into cellular component than the other two categories (Fig. 6b).

Within 155 DEGs, KEGG (Kyoto Encyclopedia of Genes and Genomes) database

202 analysis revealed 24 DEGs were relevant to metabolic pathways. The pathways related
203 to lipid metabolism were mostly enriched, including fat digestion and absorption,
204 glycosphinglipid biosynthesis, linoleic aicd metabolism and bile secretion (Fig. 6c).
205 These included a set of DEGs such as B3gnt5, Abcg8, Gyk, St8sia5, Pla2g2f, Aqp8,
206 Abcg5, Pla2g4f, Fut9, Adh1, and Cyp2c68 which were highly upregulated in colon
207 tissues from PBG-treated mice (Table S1). These findings indicated that PBG could
208 promote host lipid metabolism, regardless of gut microbiota.

Discussion

The polysaccharopeptides produced by *C. versicolor* are effective immunopotentiators, supplementing the chemotherapy and radiotherapy of caners and infectious diseases. Several kinds of polysaccharopeptides have been shown to be produced by cultured mycelia or fruiting bodies. Although some of these polymers are structurally distinct, they are not distinguishable in terms of physiological activities (27).

PBG, one representative of polysaccharopeptides from the fruiting bodies of *C. versicolor*, indeed upregulates expression of genes related to host immune response in colon tissues (Table S1). The most pronounced one is CTSE gene, which encodes cathepsin E, an aspartic endopeptidase involved in antigen processing via the MHC class II pathway (28). Besides, several sets of genes related to elements of Toll-like or NOD-like signaling pathway and the complement system are upregulated (Table S1). These data suggest that PBG can activate innate and adaptive immunity in the intestine. Paradoxically, PBG suppresses systemic metabolic inflammation in HFD-fed obese animal models (Fig.2). Further evidences showed that this was due to PBG's ability to improve intestinal barrier integrity and thus decrease leakage of microbial LPS from gut into circulation.

The modulation of the gut microbiotic composition offers a new avenue for the treatment of obesity and metabolic disorders (18). PBG is identified for the first time as an anti-obesity agent. The transfer of feces from PBG-treated mice protected the recipient HFD-fed mice from obesity, suggesting a vital role of gut microbiota in

PBG's anti-obesity effect. Unlike other established prebiotics such as dietary polyphenols (29), inulin (30), and oat-derived β-glucan (31), PBG didn't restore HFD-induced increase in the *Firmicutes* to *Bacteroidetes* ratio. PBG markedly increased the abundance of *A. muciniphila*, a mucin-degrading bacterium that could reverse HFD-induced obesity (32). PBG didn't boost the growth of *A. muciniphila*, either in pure cultures or gut-simulators. By use of a cocktail of antibiotics, microbiota-depleted mice were generated. Data from microbiota-depleted mice indicated that PBG created an intestinal microenvironment favorable for *A. muciniphila* colonization. The genome of *A. muciniphila* contains a large proportion of genes encoding secreted proteins (567 of the 2,176 open reading frames), 61 of which have been assigned protease, sugar hydrolase, sialidase, or sulfatase activities, suggesting specialization in mucus utilization and adaptation to the gut environment (33). Given recent evidence indicated that *A. muciniphila* colonization was mediated by host immune status (34, 35), it will be intriguing to clarify the relationship between richness of *A. muciniphila* and PBG-induced immunomodulation in the future.

Transcriptome analysis of PBG-induced differentially expressed genes in colon tissues indicated that PBG had a direct pronounced effect on host lipid metabolism. These finding implied that PBG might reduce fat accumulation through a microbiota-dependent or -independent manner.

In summary, we demonstrated that PBG, one representative of *C. versicolor* polysaccharopeptide originally used as an adjunct therapy for cancers could be an anti-obesity agent through modulating gut microbiota and regulating host metabolism.

253 Overweight and obesity are associated with at least 13 different types of cancer. These
254 cancers make up 40% of all cancers diagnosed (36, 37). A variety of biological
255 mechanisms involving the adipocyte has been implicated in tumorigenesis. The
256 previous consensus on the anti-cancer effect and the current knowledge in the
257 anti-obesity effect of *C. versicolor* polysaccharopeptides might make them favorable to
258 those patients suffered from obesity-associated cancers.
259

Methods

Murine

C57BL/6J female mice were purchased from the Fourth Military Medical University (Xi'an, Shaanxi, China). After one week for accommodation, mice were randomly distributed into different groups, fed with either a standard chow diet (10 kcal % Fat, D12492) or a high-fat diet (60 kcal % Fat, D12450J). Animal procedures were approved by the Animal Ethics Committee in Northwest A & F University, China.

Preparation of protein-bound β-glucan

The *Coriolus versicolor* powder was subjected to hot water extraction and alcohol precipitation. The resulting precipitates were dissolved in water and dialyzed (cutting MW at 8000 Da). The non-dialysates were concentrated and the supernatant was applied to a DEAE-Fast-Flow column (10 i.d. × 60 cm) with stepwise distilled H_2O and 0.5 M NaCl solution. The 0.5 M NaCl eluent, designated as PBG was dialyzed and lyophilized. The structural information was shown in Table S2.

Body composition analysis

Body composition was measured with the nuclear magnetic resonance system using a Body Composition Analyzer MiniQMR23-060H-I (Niumag, Shanghai, China). Body fat and lean mass were determined in live conscious mice with adlibitum access to chow as previously described (38).

H&E Staining

Liver was fixed in 10% buffered formalin at room temperature before embedding in paraffin. Histological assessment of H&E sections was performed in a blinded fashion by a pathologist using a previously described scoring system (39).

Cytokine measurements

IL-1β, IL-6, IL-10 and TNF-α protein levels in serum were measured using

285 commercial Bio-Plex Pro mouse kits (BIO-RAD, USA).

286 **Biochemical analysis**

287 Serum leptin, adiponectin, and LPS were measured by quantification assay kits
288 (Cusabio, China). Triglyceride and total BA were assayed using commercial detection
289 kits (Nanjing Jiancheng Chemical Industrial Co. Ltd, China).

290 **Real-Time PCR**

291 Samples of total RNA from colon tissue was isolated using the TRIZOL solution
292 (TransGen, Beijing, China). Quantitative real-time reverse-transcription PCR
293 (qRT-PCR) was performed in triplicate on a QuantStudio™ 6 Flex Real-Time PCR
294 (Life Technologies, Singapore). The primers used are shown in Table S3 (40, 41).

295 **Gut microbiota analysis**

296 Stool samples were snap-frozen in liquid nitrogen before storage at -80°C. Total
297 bacterial DNA was extracted using a fecal DNA isolation kit (MoBio Laboratories,
298 USA) according to the manufacturer's protocol. The 16S rRNA gene comprising
299 V3–V4 regions was amplified using common primer pair and the microbial diversity
300 analysis was performed as described (42).

301 Briefly, the raw sequences were first quality-controlled using QIIMEwith default
302 parameters, then demultiplexed and clustered into species-level (97% similarity)
303 operational taxonomic units (OTUs). OUT generation is based on GreenGene's
304 database and the reference-based method with SortMeRNA. Strain composition
305 analysis, alpha diversity analysis and beta diversity analysis were also performed using
306 QIIME. Discriminative taxa were determined using LEfSe (LDA Effect Size,
307 http://huttenhower.sph.harvard.edu/galaxy/).

308 ***In vitro* gut simulator**

309 A three compartment dynamic *in vitro* human intestinal tract model (SHIME) was

used to study the effects of PBG on a stabilized gut microbial community in a controlled *in vitro* setting (43).

A. muciniphila colonization

C57Bl/6J female mice (4 weeks old) were fed with HFD and treated with an antibiotic cocktail for 4 weeks as described (44). The microbiota-depleted mice were daily supplementated with or without PBG (400 mg/kg) for another month in the presence of antibiotics. Mice were lavaged with *A. muciniphila* (1.5×10^8 cfu) continuously for 3 days as previously described (32). Fecal samples were collected 24 h after each lavage and *Akkermansia muciniphila* in the feces was quantified by qPCR using the universal 16S rRNA gene primers (shown in Table S3).

Fecal transplantation

Fecal transplantation was performed according to a previous study (45). The donor mice (4-week-old, n=10 per group) were fed with Chow, (PBG+Chow), (PBG+HFD), or HFD for 4 weeks. Stools from donor mice of each diet group were subsequently collected and pooled. The transplant material was prepared as resuspension of 100 mg of stools from each diet group in 1 ml of sterile saline, and centrifugation at 800g for 3 min to obtain the supernatant. The recipient mice (8-week-old, n=6-8 per transplant group) were fed with HFD and orally treated with 200µl of fresh transplant material daily, which was prepared on the same day within 10 min of transplantation. After 8 weeks of treatment, the recipient mice were killed for subsequent analysis.

Transcriptomic analysis

HFD-fed mice were treated daily with a cocktail of antibiotics for one month, followed by supplementation with or without PBG (400 mg/kg) for another month in the presence of antibiotics (46). RNA extracted from colon tissues was performed via a

335 paired-end 125 cycle rapid run on the Illumina HiSeq. 2500. The clean reads that were
336 filtered from the raw reads were mapped to mouse (C57BL/6 strain) reference genome
337 (GRCm38) using Tophat2 (47) software. FPKM values were used to estimate gene
338 expression by use of the Cufflinks software (26). The DESeq (48), Kyoto
339 Encyclopaedia of Genes and Genomes (KEGG), and gene ontology (GO) terms were
340 determined via protein database by BLASTX (49).

341 **Statistical analysis**

342 All data of experiment were shown as means± standard error of mean (S.E.M.)
343 Data sets that involved more than two groups were assessed by one-way ANOVA
344 followed by Dunnett's multiple comparisons test and unpaired two-tailed Student's
345 t-test. 16S rRNA gene sequence analysis was assessed using Paired Wilcoxon
346 rank-sum test. A p value of 0.05 was considered statistically significant based on
347 ANOVA statistical analysis by Graphpad 7.0 and the R programming language. Data
348 of RNA-Sequence are presented as mean FPKM ± S.E.M.. Differences between PBG
349 and Blank mice that were evaluated FDR ($p < 0.05$) by using Benjamini-Hochberg
350 method.

351 **Acknowledgement**

352 This work was supported by the National Natural Science Foundation of China
353 (NSFC) (31570799), and Fundamental Research Funds for the Central Universities,
354 Northwest A&F University (2452017026).

355 **Competing interests**

356 The authors declare that they have no conflict of interest.

References

1. **Kopelman PG.** 2000. Obesity as a medical problem. Nature **404:**635.
2. **Dietz WH, Baur LA, Hall K, Puhl RM, Taveras EM, Uauy R, Kopelman P.** 2015. Management of obesity: improvement of health-care training and systems for prevention and care. Lancet **385:**2521-2533.
3. **Ryder JR, Fox CK, Kelly AS.** 2018. Treatment Options for Severe Obesity in the Pediatric Population: Current Limitations and Future Opportunities. Obesity **26:**951-960.
4. **Apovian CM, Garvey WT, Ryan DH.** 2015. Challenging obesity: Patient, provider, and expert perspectives on the roles of available and emerging nonsurgical therapies. Obesity **23 Suppl 2:**S1-S26.
5. **Patel D.** 2015. Pharmacotherapy for the management of obesity. Metabolism: clinical and experimental **64:**1376-1385.
6. **Srivastava G, Apovian CM.** 2018. Current pharmacotherapy for obesity. Nature reviews. Endocrinology **14:**12-24.
7. **Novac N.** 2013. Challenges and opportunities of drug repositioning. Trends in pharmacological sciences **34:**267-272.
8. **Sleire L, Forde HE, Netland IA, Leiss L, Skeie BS, Enger PO.** 2017. Drug repurposing in cancer. Pharmacological research **124:**74-91.
9. **Wurth R, Thellung S, Bajetto A, Mazzanti M, Florio T, Barbieri F.** 2016. Drug-repositioning opportunities for cancer therapy: novel molecular targets for known compounds. Drug discovery today **21:**190-199.
10. **Smith JE, Rowan NJ, Sullivan R.** 2002. Medicinal mushrooms: a rapidly developing area of biotechnology for cancer therapy and other bioactivities. Biotechnol Lett **24:**1839-1845.
11. **Yu Y, Shen M, Song Q, Xie J.** 2018. Biological activities and pharmaceutical applications of polysaccharide from natural resources: A review. Carbohydrate polymers **183:**91-101.
12. **Schepetkin IA, Quinn MT.** 2006. Botanical polysaccharides: macrophage immunomodulation and therapeutic potential. International immunopharmacology **6:**317-333.
13. **Singdevsachan SK, Auroshree P, Mishra J, Baliyarsingh B, Tayung K, Thatoi H.** 2016. Mushroom polysaccharides as potential prebiotics with their antitumor and immunomodulating properties: A review. Bioact Carbohydr Diet Fibre **7:**1-14.
14. **Saleh MH, Rashedi I, Keating A.** 2017. Immunomodulatory Properties of Coriolus versicolor: The Role of Polysaccharopeptide. Frontiers in immunology **8:**1087.
15. **Ren Y, Geng Y, Chen H, Lu Z-M, Shi J-S, Xu Z.** 2018. Polysaccharide peptides from Coriolus versicolor: A multi-targeted approach for the protection or prevention of alcoholic liver disease. J Funct Foods **40:**769-777.
16. **Armitage J.** 2007. The safety of statins in clinical practice. Lancet **370:**1781-1790.
17. **Stephens RW, Arhire L, Covasa M.** 2018. Gut Microbiota: From Microorganisms to Metabolic Organ Influencing Obesity. Obesity **26:**801-809.
18. **Cani PD, Delzenne NM.** 2009. Interplay between obesity and associated metabolic disorders: new insights into the gut microbiota. Curr Opin Pharmacol **9:**737-743.
19. **Dao MC, Clement K.** 2018. Gut microbiota and obesity: Concepts relevant to clinical care. European journal of internal medicine **48:**18-24.
20. **Ley RE, Turnbaugh PJ, Klein S, Gordon JI.** 2006. Microbial ecology: human gut microbes associated with obesity. Nature **444:**1022-1023.

21. **Derrien M, Belzer C, de Vos WM.** 2017. Akkermansia muciniphila and its role in regulating host functions. Microbial pathogenesis **106:**171-181.
22. **Graziani F, Pujol A, Nicoletti C, Dou S, Maresca M, Giardina T, Fons M, Perrier J.** 2016. Ruminococcus gnavus E1 modulates mucin expression and intestinal glycosylation. Journal of applied microbiology **120:**1403-1417.
23. **Pinton P, Graziani F, Pujol A, Nicoletti C, Paris O, Ernouf P, Di Pasquale E, Perrier J, Oswald IP, Maresca M.** 2015. Deoxynivalenol inhibits the expression by goblet cells of intestinal mucins through a PKR and MAP kinase dependent repression of the resistin-like molecule beta. Molecular nutrition & food research **59:**1076-1087.
24. **Bergstrom KS, Xia L.** 2013. Mucin-type O-glycans and their roles in intestinal homeostasis. Glycobiology **23:**1026-1037.
25. **Tremaroli V, Bäckhed F.** 2012. Functional interactions between the gut microbiota and host metabolism. Nature **489:**242.
26. **Trapnell C, Williams BA, Pertea G, Mortazavi A, Kwan G, van Baren MJ, Salzberg SL, Wold BJ, Pachter L.** 2010. Transcript assembly and quantification by RNA-Seq reveals unannotated transcripts and isoform switching during cell differentiation. Nature biotechnology **28:**511-515.
27. **Cui J, Chisti Y.** 2003. Polysaccharopeptides of Coriolus versicolor: physiological activity, uses, and production. Biotechnology advances **21:**109-122.
28. **Zaidi N, Kalbacher H.** 2008. Cathepsin E: a mini review. Biochemical and biophysical research communications **367:**517-522.
29. **Roopchand DE, Carmody RN, Kuhn P, Moskal K, Rojas-Silva P, Turnbaugh PJ, Raskin I.** 2015. Dietary Polyphenols Promote Growth of the Gut Bacterium Akkermansia muciniphila and Attenuate High-Fat Diet-Induced Metabolic Syndrome. Diabetes **64:**2847-2858.
30. **Han KH, Yamamoto A, Shimada KI, Kikuchi H, Fukushima M.** 2017. Dietary fat content modulates the hypolipidemic effect of dietary inulin in rats. Molecular nutrition & food research **61:**1600635.
31. **Luo Y, Zhang L, Li H, Smidt H, Wright AG, Zhang K, Ding X, Zeng Q, Bai S, Wang J, Li J, Zheng P, Tian G, Cai J, Chen D.** 2017. Different Types of Dietary Fibers Trigger Specific Alterations in Composition and Predicted Functions of Colonic Bacterial Communities in BALB/c Mice. Frontiers in microbiology **8:**966.
32. **Everard A, Belzer C, Geurts L, Ouwerkerk JP, Druart C, Bindels LB, Guiot Y, Derrien M, Muccioli GG, Delzenne NM, de Vos WM, Cani PD.** 2013. Cross-talk between *Akkermansia muciniphila* and intestinal epithelium controls diet-induced obesity. Proc Natl Acad Sci USA **110:**9066-9071.
33. **van Passel MW, Kant R, Zoetendal EG, Plugge CM, Derrien M, Malfatti SA, Chain PS, Woyke T, Palva A, de Vos WM, Smidt H.** 2011. The genome of Akkermansia muciniphila, a dedicated intestinal mucin degrader, and its use in exploring intestinal metagenomes. PloS one **6:**e16876.
34. **Greer RL, Dong X, Moraes AC, Zielke RA, Fernandes GR, Peremyslova E, Vasquez-Perez S, Schoenborn AA, Gomes EP, Pereira AC, Ferreira SR, Yao M, Fuss IJ, Strober W, Sikora AE, Taylor GA, Gulati AS, Morgun A, Shulzhenko N.** 2016. Akkermansia muciniphila mediates negative effects of IFNgamma on glucose metabolism. Nature communications **7:**13329.
35. **Seregin SS, Golovchenko N, Schaf B, Chen J, Pudlo NA, Mitchell J, Baxter NT, Zhao L, Schloss PD, Martens EC, Eaton KA, Chen GY.** 2017. NLRP6 Protects Il10(-/-) Mice from Colitis by Limiting Colonization of Akkermansia muciniphila. Cell reports **19:**2174.
36. **Steele CB, Thomas CC, Henley SJ, Massetti GM, Galuska DA, Agurs-Collins T, Puckett M, Richardson LC.** 2017. Vital Signs: Trends in Incidence of Cancers Associated with Overweight and

Obesity - United States, 2005-2014. MMWR. Morbidity and mortality weekly report **66:**1052-1058.

37. **Pearson-Stuttard J, Zhou B, Kontis V, Bentham J, Gunter MJ, Ezzati M.** 2018. Worldwide burden of cancer attributable to diabetes and high body-mass index: a comparative risk assessment. The lancet. Diabetes & endocrinology **6:**e6-e15.
38. **Chen X, Zhang F, Gong Q, Cui A, Zhuo S, Hu Z, Han Y, Gao J, Sun Y, Liu Z, Yang Z, Le Y, Gao X, Dong LQ, Gao X, Li Y.** 2016. Hepatic ATF6 Increases Fatty Acid Oxidation to Attenuate Hepatic Steatosis in Mice Through Peroxisome Proliferator–Activated Receptor α. Diabetes **65:**1904.
39. **Nakamura A, Tajima K, Zolzaya K, Sato K, Inoue R, Yoneda M, Fujita K, Nozaki Y, Kubota KC, Haga H, Kubota N, Nagashima Y, Nakajima A, Maeda S, Kadowaki T, Terauchi Y.** 2012. Protection from non-alcoholic steatohepatitis and liver tumourigenesis in high fat-fed insulin receptor substrate-1-knockout mice despite insulin resistance. Diabetologia **55:**3382-3391.
40. **Guo X, Zhang J, Wu F, Zhang M, Yi M, Peng Y.** 2016. Different subtype strains of Akkermansia muciniphila abundantly colonize in southern China. Journal of applied microbiology **120:**452-459.
41. **Wlodarska M, Luo C, Kolde R, d'Hennezel E, Annand JW, Heim CE, Krastel P, Schmitt EK, Omar AS, Creasey EA, Garner AL, Mohammadi S, O'Connell DJ, Abubucker S, Arthur TD, Franzosa EA, Huttenhower C, Murphy LO, Haiser HJ, Vlamakis H, Porter JA, Xavier RJ.** 2017. Indoleacrylic Acid Produced by Commensal Peptostreptococcus Species Suppresses Inflammation. Cell host & microbe **22:**25-37 e26.
42. **Qin J, Li Y, Cai Z, Li S, Zhu J, Zhang F, Liang S, Zhang W, Guan Y, Shen D, Peng Y, Zhang D, Jie Z, Wu W, Qin Y, Xue W, Li J, Han L, Lu D, Wu P, Dai Y, Sun X, Li Z, Tang A, Zhong S, Li X, Chen W, Xu R, Wang M, Feng Q, Gong M, Yu J, Zhang Y, Zhang M, Hansen T, Sanchez G, Raes J, Falony G, Okuda S, Almeida M, LeChatelier E, Renault P, Pons N, Batto JM, Zhang Z, Chen H, Yang R, Zheng W, Li S, Yang H, Wang J, Ehrlich SD, Nielsen R, Pedersen O, Kristiansen K, Wang J.** 2012. A metagenome-wide association study of gut microbiota in type 2 diabetes. Nature **490:**55-60.
43. **Wu H, Esteve E, Tremaroli V, Khan MT, Caesar R, Manneras-Holm L, Stahlman M, Olsson LM, Serino M, Planas-Felix M, Xifra G, Mercader JM, Torrents D, Burcelin R, Ricart W, Perkins R, Fernandez-Real JM, Backhed F.** 2017. Metformin alters the gut microbiome of individuals with treatment-naive type 2 diabetes, contributing to the therapeutic effects of the drug. Nature medicine **23:**850-858.
44. **Grivennikov SI, Wang K, Mucida D, Stewart CA, Schnabl B, Jauch D, Taniguchi K, Yu GY, Osterreicher CH, Hung KE, Datz C, Feng Y, Fearon ER, Oukka M, Tessarollo L, Coppola V, Yarovinsky F, Cheroutre H, Eckmann L, Trinchieri G, Karin M.** 2012. Adenoma-linked barrier defects and microbial products drive IL-23/IL-17-mediated tumour growth. Nature **491:**254-258.
45. **Li G, Xie C, Lu S, Nichols RG, Tian Y, Li L, Patel D, Ma Y, Brocker CN, Yan T, Krausz KW, Xiang R, Gavrilova O, Patterson AD, Gonzalez FJ.** 2017. Intermittent Fasting Promotes White Adipose Browning and Decreases Obesity by Shaping the Gut Microbiota. Cell metabolism **26:**801.
46. **Fu ZD, Selwyn FP, Cui JY, Klaassen CD.** 2017. RNA-Seq Profiling of Intestinal Expression of Xenobiotic Processing Genes in Germ-Free Mice. Drug metabolism and disposition: the biological fate of chemicals **45:**1225-1238.
47. **Kim D, Pertea G, Trapnell C, Pimentel H, Kelley R, Salzberg SL.** 2013. TopHat2: accurate alignment of transcriptomes in the presence of insertions, deletions and gene fusions. Genome biology **14:**R36.
48. **Anders S, Huber W.** 2010. Differential expression analysis for sequence count data. Genome biology **11:**R106.

489 49. **Conesa A, Gotz S, Garcia-Gomez JM, Terol J, Talon M, Robles M.** 2005. Blast2GO: a universal tool
490 for annotation, visualization and analysis in functional genomics research. Bioinformatics
491 **21:**3674-3676.

492

493

494 **Figure legends**

495 **Fig.1. PBG treatment decreases body weight and fat accumulation in**
496 **HFD-induced obese mice.** HFD-fed mice were treated daily with either water (group
497 HFD), simvastatin at 2 mg/kg (Group P) or PBG at 200 (Group L) or 400 mg/kg
498 (Group H) by intragastric gavage for 9 weeks (n=11-13 for each group). As a control,
499 Chow-fed mice (Group Chow) were lavaged with water daily. (a) body weight curves;
500 (b) body weight gain; (c) liver weight; (d) food consumption; (e) fat mass; (f) lean
501 mass; (g) a representative of magnetic resonance imaging (MRI); (h) fat area by MRI;
502 (i) serum triglyceride; (j) total bile acid in serum; (k) serum leptin; (l) serum
503 adiponectin; (m) a representative of liver sections in which lipid content was assessed
504 using H&E staining; (h) normalized fold change of liver lipid content. Data are shown
505 as mean±s.e.m. *p* value in (a) and (l) were analysed using unpaired two-tailed
506 Student's t-test. *p* value in (b)-(k) and (n) were analysed using Dunnett's multiple
507 comparisons test. *$p < 0.05$, **$p < 0.01$, ***$p < 0.001$ and ****$p < 0.0001$.

508 **Fig.2. PBG treatment reduces serum pro-inflammation cytokines and**
509 **lipopolysaccharide through improvement of intestinal barrier integrity in obese**
510 **mice.** Mice were treated as Figure 1. Effects of PBG treatment on serum TNF-α, IL-1β,
511 IL-17A, IL-6 and endotoxin **(**a-e**)** were examined by ELISA kits, and on relative
512 mRNA expression of ZO-1(f) and occludin (g) in colon were assessed using qRT-PCR;
513 (h) relative mRNA expression of ZO-1 and occludin from colons of mirobiota-depleted
514 mice treated with or without PBG. *p* value in (a-e) were analysed using Dunnett's
515 multiple comparisons test. *p* value in (f-h) were analyzed using unpaired two-tailed

516 Student's t-test. *$p < 0.05$, **$p < 0.01$, ***$p < 0.001$,****$p < 0.0001$.

517 **Fig.3. PBG treatment affects mcirobiota in HFD-induced obese mice.**

518 Microbiota composition were analyzed using a pyrosequencing-based assay on feces of
519 chow- and HFD-fed mice (n=11-13 for each group) as described in Figure 1. (a) Plots
520 were generated using the unweighted version of the UniFrac-based PcoA; (b) Bacterial
521 taxonomic profiling in the phylum level of microbiota from individual groups; (c)
522 Comparison of *Firmicutes* to *Bacteroidetes* ratio and relative abundance of the phylm
523 *Verrucomicrobia*. *p* values were analyzed using Dunnett's multiple comparisons test
524 (*$p < 0.05$, **$p < 0.01$, ***$p < 0.001$, ****$p < 0.0001$). (d) Heatmap and bacterial taxa
525 information (genus, family and phylum) of the Top 100 OTUs. Difference was
526 analyzed using Paired Wilcoxon rank-sum test (*$p < 0.05$).

527 **Fig.4. Effects of PBG on *A. muciniphila* growth and colonization as well as gene**
528 **expression of intestinal mucin 2.** (a) Growth of *A. muciniphila* as a single culture in
529 the presence or absence of 10-mM PBG (with six technical replicates); (b) Growth of *A.*
530 *muciniphila* in complex microbiota using the *in vitro* gut simulator with or without
531 PBG exposure; (c) Effects of PBG treatment on *A. muciniphila* colonization in
532 microbiota-depleted mice. HFD-fed mice were treated daily with a cocktail of
533 antibiotics for one month, followed by supplementation with or without PBG (400
534 mg/kg) for another month in the presence of antibiotics. Mice were lavaged with *A.*
535 *muciniphila* (1.5×10^8 cfu) continuously for 3 days. *A. muciniphila* in the fecal
536 samples was determined 24 h after each lavage; (d) Effects of PBG treatment on gene
537 expression of protein and glycosyltransferases of mucin 2 in the colon tissues from

538 microbiota-depleted mice. *p* value was analyzed using unpaired two-tailed Student's
539 t-test (*$p < 0.05$).

540 **Fig.5. Obesity and related metabolic inflammation were reversed by fecal**
541 **transplantation from PBG-treated mice to HFD-fed mice.** HFD-fed mice were
542 colonized with feces from different mouse groups for 8 weeks (n=6-8 for each group),
543 followed by measurement of body weight (a), total bile acid (b), serum adiponectin (c),
544 leptin (d), IL-6 (e), IL-1β (f), and TNF-α (g). *p* value in (a) and (c) were analyzed using
545 unpaired two-tailed Student's t-test. *p* value in (b) and (d)-(g) were analyzed using
546 Dunnett's multiple comparisons test. *$p < 0.05$, **$p < 0.01$, ***$p < 0.001$,****$p <$
547 0.0001.

548 **Fig.6. Transcriptome analysis of differentially expressed genes (DEGs) in colon**
549 **tissues of microbiota-depleted mice treated with or without PBG.** HFD-fed mice
550 were treated daily with a cocktail of antibiotics for one month, followed by
551 supplementation with or without PBG (400 mg/kg) for another month in the presence
552 of antibiotics. (a) heatmap of total 155 DEGs; (b) Gene Ontology (GO) assignments of
553 DEGs; (c) KEGG enrichment analysis of PBG-induced upregulated DEGs. The top 20
554 pathways were shown. The x-axis indicates the enrichment factor, and the y-axis shows
555 the KEGG pathway.

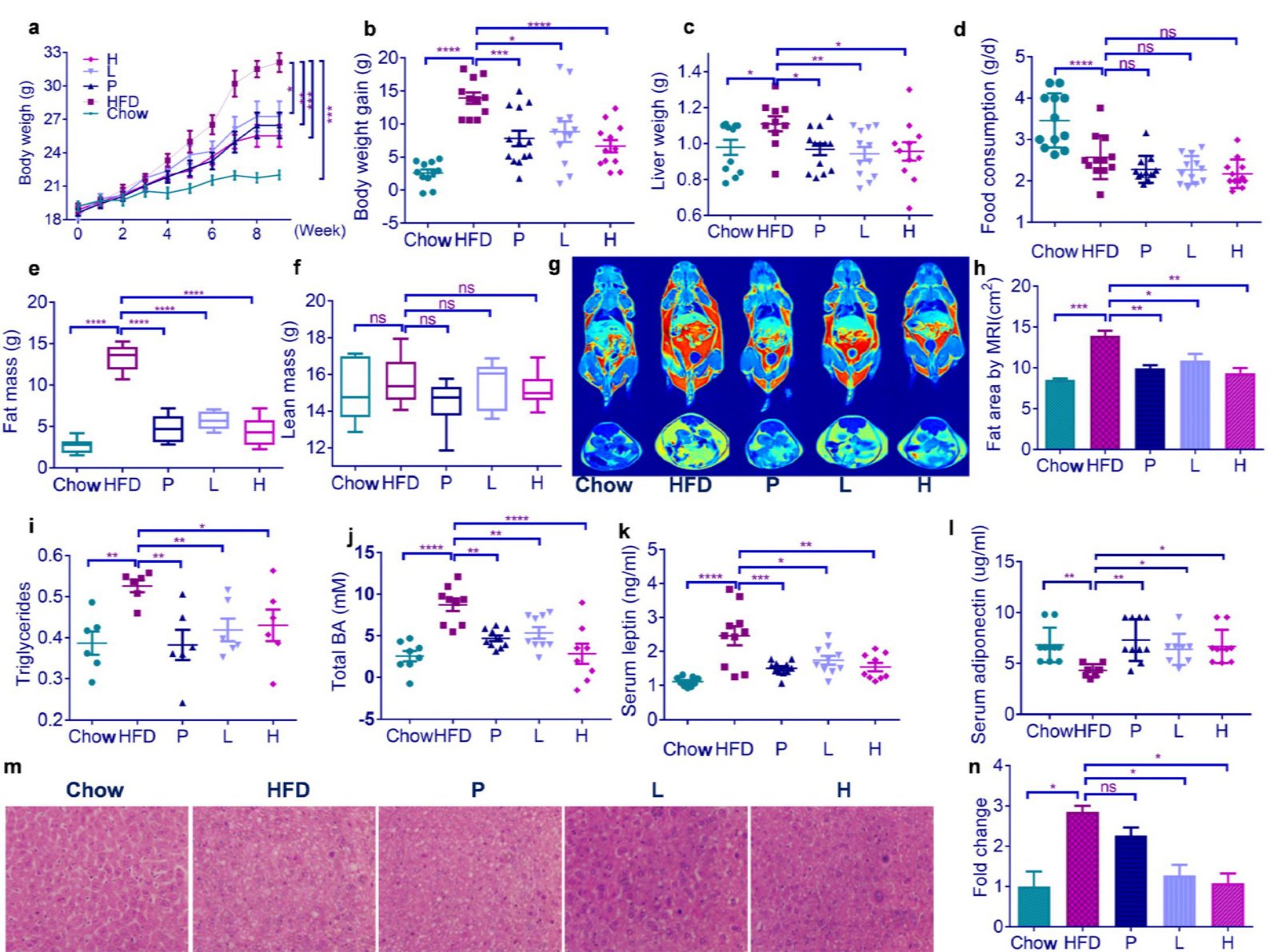
a
Body weigh (g)
H
L
P
HFD
Chow
(Week)
b
Body weight gain (g)
Chow HFD P L H
c
Liver weigh (g)
Chow HFD P L H
d
Food consumption (g/d)
ns
Chow HFD P L H
e
Fat mass (g)
Chow HFD P L H
f
Lean mass (g)
ns
Chow HFD P L H
g
Chow
HFD
P
L
H
h
Fat area by MRI(cm2)
Chow HFD P L H
i
Triglycerides
Chow HFD P L H
j
Total BA (mM)
Chow HFD P L H
k
Serum leptin (ng/ml)
Chow HFD P L H
l
Serum adiponectin (ug/ml)
Chow HFD P L H
m
Chow
HFD
P
L
H
n
Fold change
Chow HFD P L H

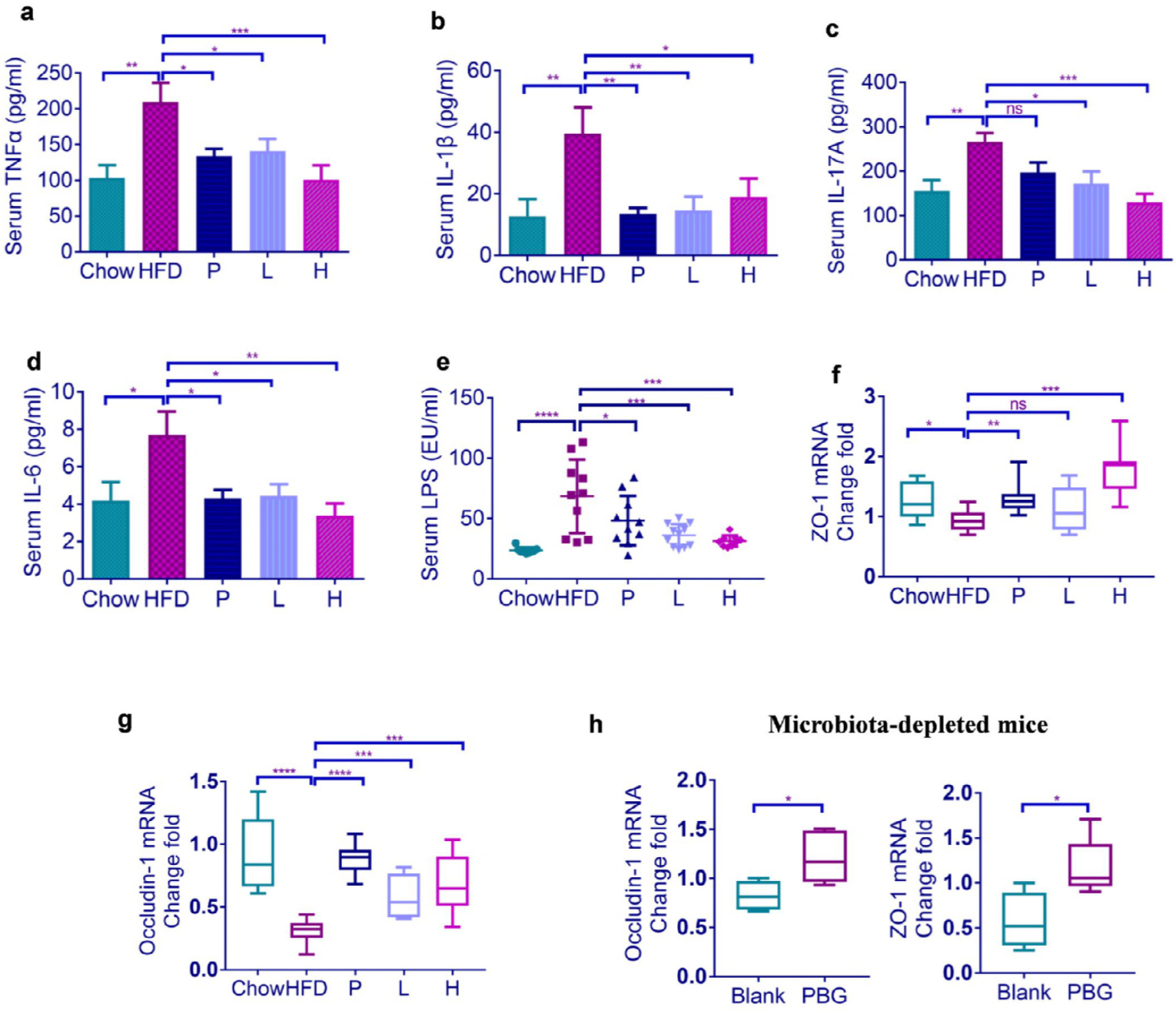
a
Serum TNFα (pg/ml)
250
200
150
100
50
0
Chow HFD P L H
b
Serum IL-1β (pg/ml)
60
40
20
0
Chow HFD P L H
c
Serum IL-17A (pg/ml)
400
300
200
100
0
ns
Chow HFD P L H
d
Serum IL-6 (pg/ml)
10
8
6
4
2
0
Chow HFD P L H
e
Serum LPS (EU/ml)
150
100
50
0
Chow HFD P L H
f
ZO-1 mRNA Change fold
3
2
1
0
ns
Chow HFD P L H
g
Occludin-1 mRNA Change fold
1.5
1.0
0.5
0.0
Chow HFD P L H
h
Microbiota-depleted mice
Occludin-1 mRNA Change fold
2.0
1.5
1.0
0.5
0.0
Blank PBG
ZO-1 mRNA Change fold
2.0
1.5
1.0
0.5
0.0
Blank PBG

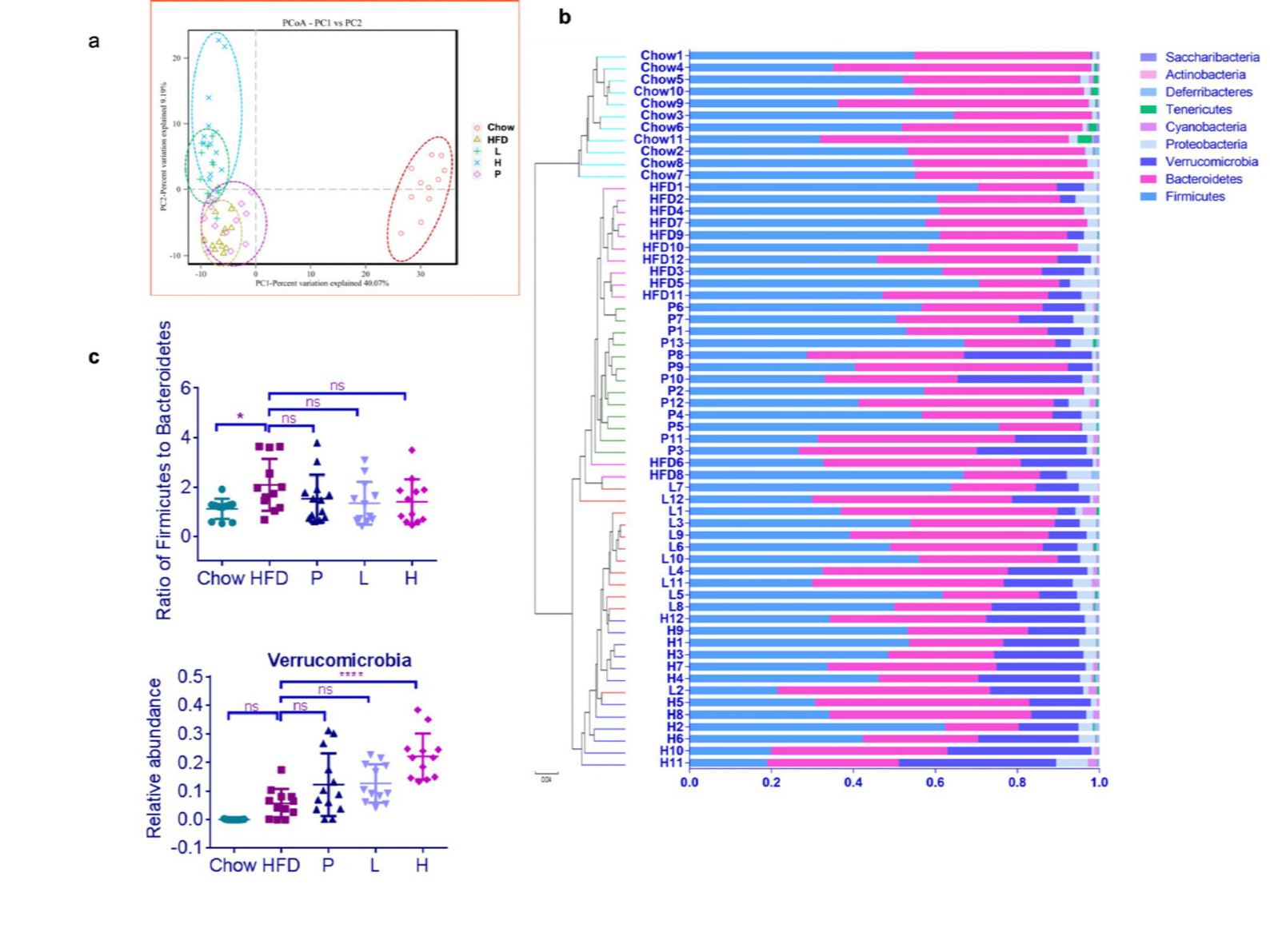
a
PCoA - PC1 vs PC2
PC2-Percent variation explained 9.19%
PC1-Percent variation explained 40.07%
Chow
HFD
L
H
P
b
Saccharibacteria
Actinobacteria
Deferribacteres
Tenericutes
Cyanobacteria
Proteobacteria
Verrucomicrobia
Bacteroidetes
Firmicutes
Chow1
Chow4
Chow5
Chow10
Chow9
Chow3
Chow6
Chow11
Chow2
Chow8
Chow7
HFD1
HFD2
HFD4
HFD7
HFD9
HFD10
HFD12
HFD3
HFD5
HFD11
P6
P7
P1
P13
P8
P9
P10
P2
P12
P4
P5
P11
P3
HFD6
HFD8
L7
L12
L1
L3
L9
L6
L10
L4
L11
L5
L8
H12
H9
H1
H3
H7
H4
L2
H5
H8
H2
H6
H10
H11
0.0
0.2
0.4
0.6
0.8
1.0
c
Ratio of Firmicutes to Bacteroidetes
Chow HFD P L H
ns
*
Verrucomicrobia
Relative abundance
****

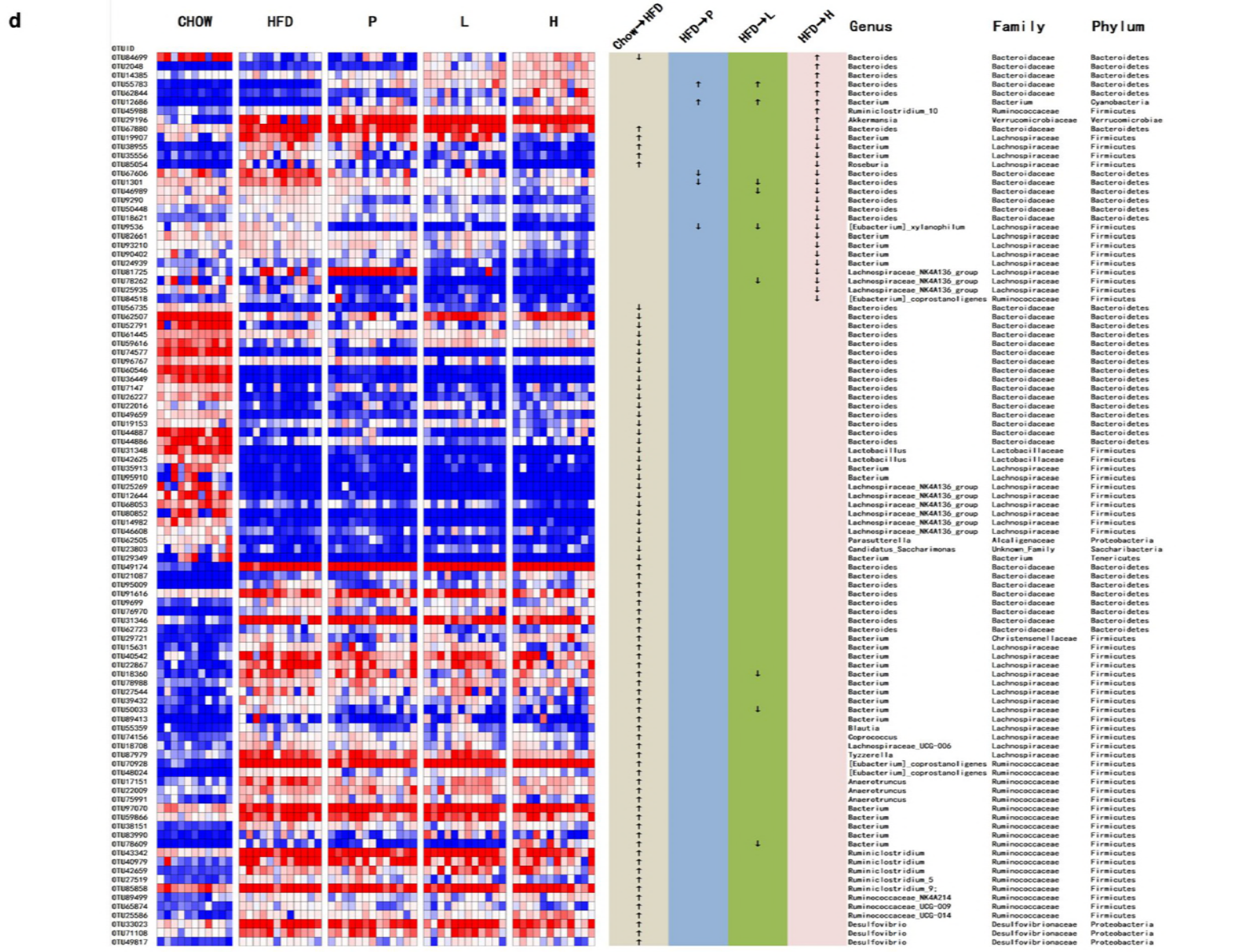
d
CHOW
HFD
P
L
H
Chow→HFD
HFD→P
HFD→L
HFD→H
Genus
Family
Phylum
OTUID
OTU84699 Bacteroides Bacteroidaceae Bacteroidetes
OTU2048 Bacteroides Bacteroidaceae Bacteroidetes
OTU14385 Bacteroides Bacteroidaceae Bacteroidetes
OTU55783 Bacteroides Bacteroidaceae Bacteroidetes
OTU62844 Bacteroides Bacteroidaceae Bacteroidetes
OTU12686 Bacterium Bacterium Cyanobacteria
OTU45988 Ruminiclostridium_10 Ruminococcaceae Firmicutes
OTU29196 Akkermansia Verrucomicrobiaceae Verrucomicrobiae
OTU67880 Bacteroides Bacteroidaceae Bacteroidetes
OTU19907 Bacterium Lachnospiraceae Firmicutes
OTU38955 Bacterium Lachnospiraceae Firmicutes
OTU35556 Bacterium Lachnospiraceae Firmicutes
OTU85054 Roseburia Lachnospiraceae Firmicutes
OTU67606 Bacteroides Bacteroidaceae Bacteroidetes
OTU1301 Bacteroides Bacteroidaceae Bacteroidetes
OTU46989 Bacteroides Bacteroidaceae Bacteroidetes
OTU9290 Bacteroides Bacteroidaceae Bacteroidetes
OTU50448 Bacteroides Bacteroidaceae Bacteroidetes
OTU18621 Bacteroides Bacteroidaceae Bacteroidetes
OTU9536 [Eubacterium]_xylanophilum Lachnospiraceae Firmicutes
OTU82661 Bacterium Lachnospiraceae Firmicutes
OTU93210 Bacterium Lachnospiraceae Firmicutes
OTU90402 Bacterium Lachnospiraceae Firmicutes
OTU24939 Bacterium Lachnospiraceae Firmicutes
OTU81725 Lachnospiraceae_NK4A136_group Lachnospiraceae Firmicutes
OTU78262 Lachnospiraceae_NK4A136_group Lachnospiraceae Firmicutes
OTU25935 Lachnospiraceae_NK4A136_group Lachnospiraceae Firmicutes
OTU84518 [Eubacterium]_coprostanoligenes Ruminococcaceae Firmicutes
OTU56735 Bacteroides Bacteroidaceae Bacteroidetes
OTU62507 Bacteroides Bacteroidaceae Bacteroidetes
OTU52791 Bacteroides Bacteroidaceae Bacteroidetes
OTU61445 Bacteroides Bacteroidaceae Bacteroidetes
OTU59616 Bacteroides Bacteroidaceae Bacteroidetes
OTU74577 Bacteroides Bacteroidaceae Bacteroidetes
OTU96767 Bacteroides Bacteroidaceae Bacteroidetes
OTU60546 Bacteroides Bacteroidaceae Bacteroidetes
OTU36449 Bacteroides Bacteroidaceae Bacteroidetes
OTU7147 Bacteroides Bacteroidaceae Bacteroidetes
OTU26227 Bacteroides Bacteroidaceae Bacteroidetes
OTU22016 Bacteroides Bacteroidaceae Bacteroidetes
OTU49659 Bacteroides Bacteroidaceae Bacteroidetes
OTU19153 Bacteroides Bacteroidaceae Bacteroidetes
OTU44887 Bacteroides Bacteroidaceae Bacteroidetes
OTU44886 Bacteroides Bacteroidaceae Bacteroidetes
OTU31348 Lactobacillus Lactobacillaceae Firmicutes
OTU42625 Lactobacillus Lactobacillaceae Firmicutes
OTU35913 Bacterium Lachnospiraceae Firmicutes
OTU95910 Bacterium Lachnospiraceae Firmicutes
OTU25269 Lachnospiraceae_NK4A136_group Lachnospiraceae Firmicutes
OTU12644 Lachnospiraceae_NK4A136_group Lachnospiraceae Firmicutes
OTU68053 Lachnospiraceae_NK4A136_group Lachnospiraceae Firmicutes
OTU80852 Lachnospiraceae_NK4A136_group Lachnospiraceae Firmicutes
OTU14982 Lachnospiraceae_NK4A136_group Lachnospiraceae Firmicutes
OTU46608 Lachnospiraceae_NK4A136_group Lachnospiraceae Firmicutes
OTU62505 Parasutterella Alcaligenaceae Proteobacteria
OTU23803 Candidatus_Saccharimonas Unknown_Family Saccharibacteria
OTU29349 Bacterium Bacterium Tenericutes
OTU49174 Bacteroides Bacteroidaceae Bacteroidetes
OTU21087 Bacteroides Bacteroidaceae Bacteroidetes
OTU95009 Bacteroides Bacteroidaceae Bacteroidetes
OTU91616 Bacteroides Bacteroidaceae Bacteroidetes
OTU9699 Bacteroides Bacteroidaceae Bacteroidetes
OTU76970 Bacteroides Bacteroidaceae Bacteroidetes
OTU31346 Bacteroides Bacteroidaceae Bacteroidetes
OTU62723 Bacteroides Bacteroidaceae Bacteroidetes
OTU29721 Bacterium Christensenellaceae Firmicutes
OTU15631 Bacterium Lachnospiraceae Firmicutes
OTU40542 Bacterium Lachnospiraceae Firmicutes
OTU22867 Bacterium Lachnospiraceae Firmicutes
OTU18360 Bacterium Lachnospiraceae Firmicutes
OTU78988 Bacterium Lachnospiraceae Firmicutes
OTU27544 Bacterium Lachnospiraceae Firmicutes
OTU39432 Bacterium Lachnospiraceae Firmicutes
OTU50033 Bacterium Lachnospiraceae Firmicutes
OTU89413 Bacterium Lachnospiraceae Firmicutes
OTU55359 Blautia Lachnospiraceae Firmicutes
OTU74156 Coprococcus Lachnospiraceae Firmicutes
OTU18708 Lachnospiraceae_UCG-006 Lachnospiraceae Firmicutes
OTU87979 Tyzzerella Lachnospiraceae Firmicutes
OTU70928 [Eubacterium]_coprostanoligenes Ruminococcaceae Firmicutes
OTU48024 [Eubacterium]_coprostanoligenes Ruminococcaceae Firmicutes
OTU17151 Anaerotruncus Ruminococcaceae Firmicutes
OTU22009 Anaerotruncus Ruminococcaceae Firmicutes
OTU75991 Anaerotruncus Ruminococcaceae Firmicutes
OTU97070 Bacterium Ruminococcaceae Firmicutes
OTU59866 Bacterium Ruminococcaceae Firmicutes
OTU38151 Bacterium Ruminococcaceae Firmicutes
OTU83990 Bacterium Ruminococcaceae Firmicutes
OTU78609 Bacterium Ruminococcaceae Firmicutes
OTU43342 Ruminiclostridium Ruminococcaceae Firmicutes
OTU40979 Ruminiclostridium Ruminococcaceae Firmicutes
OTU42659 Ruminiclostridium Ruminococcaceae Firmicutes
OTU27519 Ruminiclostridium_5 Ruminococcaceae Firmicutes
OTU85858 Ruminiclostridium_9; Ruminococcaceae Firmicutes
OTU89499 Ruminococcaceae_NK4A214 Ruminococcaceae Firmicutes
OTU65874 Ruminococcaceae_UCG-009 Ruminococcaceae Firmicutes
OTU25586 Ruminococcaceae_UCG-014 Ruminococcaceae Firmicutes
OTU33023 Desulfovibrio Desulfovibrionaceae Proteobacteria
OTU71108 Desulfovibrio Desulfovibrionaceae Proteobacteria
OTU49817 Desulfovibrio Desulfovibrionaceae Proteobacteria

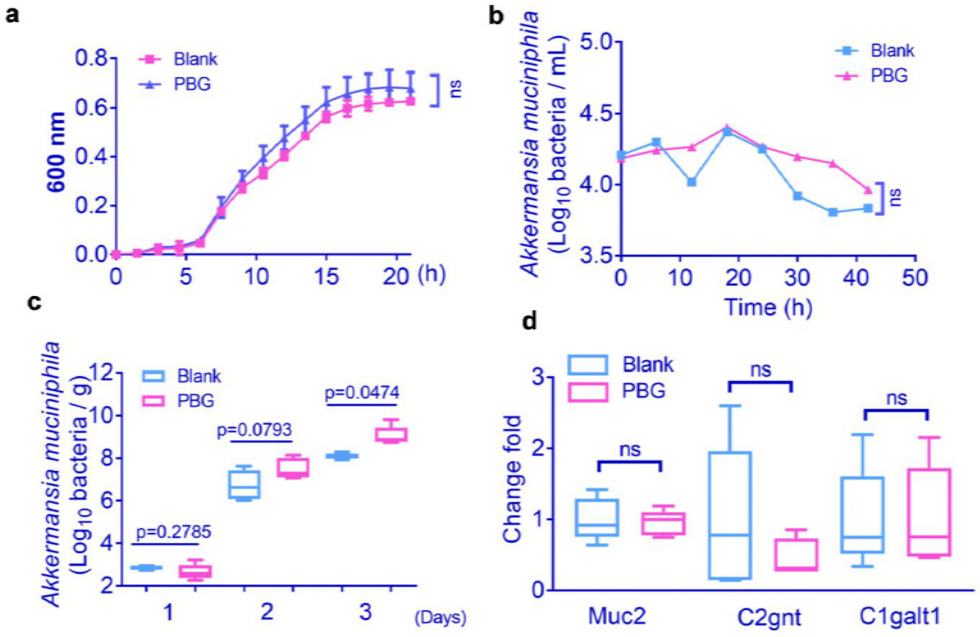
a
600 nm
Blank
PBG
ns
(h)
b
Akkermansia muciniphila
(Log10 bacteria / mL)
Blank
PBG
ns
Time (h)
c
Akkermansia muciniphila
(Log10 bacteria / g)
Blank
PBG
p=0.2785
p=0.0793
p=0.0474
(Days)
d
Change fold
Blank
PBG
ns
ns
ns
Muc2
C2gnt
C1galt1

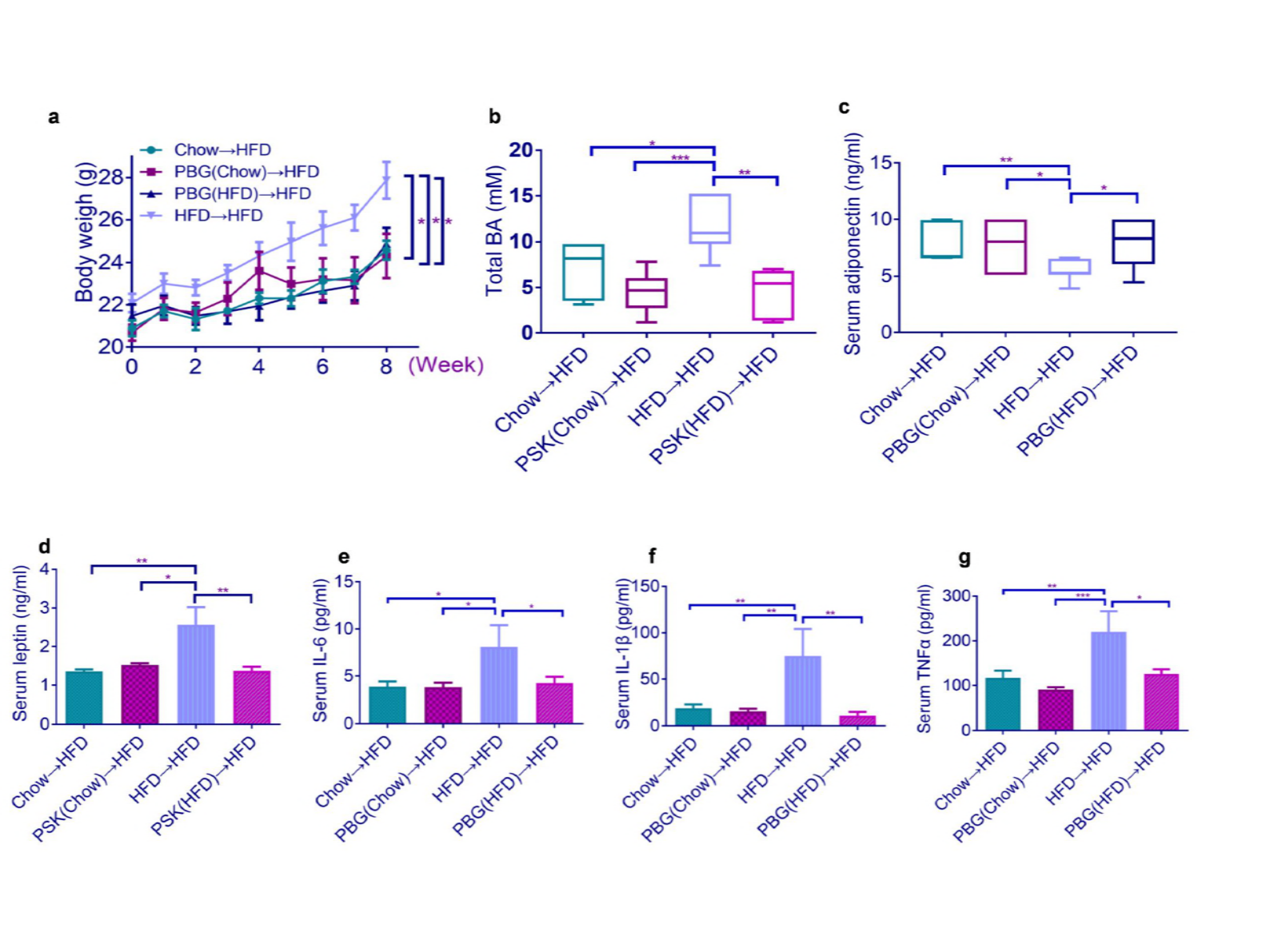
a
Chow→HFD
PBG(Chow)→HFD
PBG(HFD)→HFD
HFD→HFD
Body weigh (g)
(Week)
b
Total BA (mM)
Chow→HFD
PSK(Chow)→HFD
HFD→HFD
PSK(HFD)→HFD
c
Serum adiponectin (ng/ml)
Chow→HFD
PBG(Chow)→HFD
HFD→HFD
PBG(HFD)→HFD
d
Serum leptin (ng/ml)
Chow→HFD
PSK(Chow)→HFD
HFD→HFD
PSK(HFD)→HFD
e
Serum IL-6 (pg/ml)
Chow→HFD
PBG(Chow)→HFD
HFD→HFD
PBG(HFD)→HFD
f
Serum IL-1β (pg/ml)
Chow→HFD
PBG(Chow)→HFD
HFD→HFD
PBG(HFD)→HFD
g
Serum TNFα (pg/ml)
Chow→HFD
PBG(Chow)→HFD
HFD→HFD
PBG(HFD)→HFD

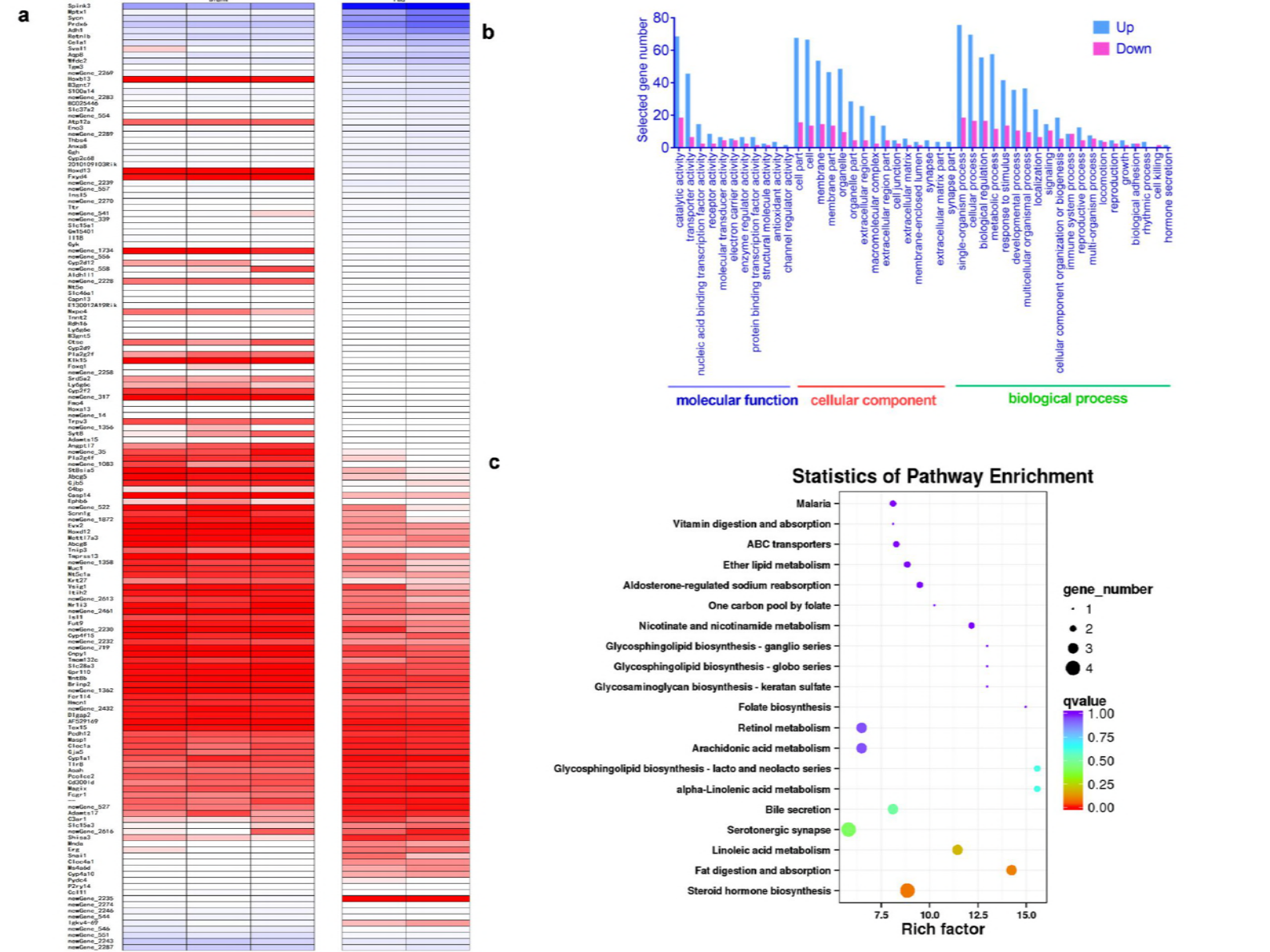
a
b
Selected gene number
Up
Down
molecular function
cellular component
biological process
c
Statistics of Pathway Enrichment
Malaria
Vitamin digestion and absorption
ABC transporters
Ether lipid metabolism
Aldosterone-regulated sodium reabsorption
One carbon pool by folate
Nicotinate and nicotinamide metabolism
Glycosphingolipid biosynthesis - ganglio series
Glycosphingolipid biosynthesis - globo series
Glycosaminoglycan biosynthesis - keratan sulfate
Folate biosynthesis
Retinol metabolism
Arachidonic acid metabolism
Glycosphingolipid biosynthesis - lacto and neolacto series
alpha-Linolenic acid metabolism
Bile secretion
Serotonergic synapse
Linoleic acid metabolism
Fat digestion and absorption
Steroid hormone biosynthesis
Rich factor
gene_number
qvalue